




Effect of extrusion ratio on the grain refinement and properties of copper prepared by powder metallurgy route

A. Mehdi¹, M. Dixit¹,  M. Agarwal² , 

¹ B.N. College of Engineering and Technology, Lucknow, India

² Dr. RML Avadh University, Faizabad, India

✉ manish.dixit39@gmail.com

ABSTRACT

The present study emphasizes determining the optimum value of the extrusion ratio for superior microstructure and mechanical properties of copper via the synergistic effect of powder metallurgy and extrusion process. In this study, sintered Cu is hot extruded for different extrusion ratios, from 2.8 to 11.1. During extrusion treatment, copper experiences high compressive and shear stress, which enhances the nucleation rate and recrystallization. It also breaks the oxide precipitates into tiny pieces with uniform dispersion. Experimental evaluation of the extruded copper pallets analyzes the effect of extrusion ratio on compressive stress, density, micro-indentation hardness, and electrical conductivity for extruded copper components. These properties show a combined effect of grain refinement and compaction as a function and potential candidate for extrusion ratio. The impact of grain refinement as a function of extrusion ratio and compressive deformation is analyzed according to microstructural analysis and different phase identification.

KEYWORDS

copper • hot extrusion • powder metallurgy • microstructure • metallurgical properties

Acknowledgements. The authors would like to acknowledge Sarda Metal Industries Jaipur for the powder materials used in the experiments. The authors also like to thank Mr. Abhilash Bajpai Center of Nano-sciences IIT Kanpur for their assistance during the work.

Citation: Mehdi A, Dixit M, Agarwal M. Effect of extrusion ratio on the grain refinement and properties of copper prepared by powder metallurgy route. 2024;52(2): 38–48.

http://dx.doi.org/10.18149/MPM.5222024_4

Introduction

Copper is a highly sought-after standout material in electrical applications including current-conducting wires, heat sinks, automotive, electric appliances, electronic devices, and other power transmission devices [1]. The high electrical conductivity, thermal conductivity, and corrosion resistance of copper make it useful in power transmission and heating applications [2,3]. The copper synthesized by the powder metallurgy route exhibits large porosity content [4,5]. It may adversely affect the physical properties of copper.

Thus, secondary processing techniques such as hot extrusion and forging may overcome these limitations. These may considerably enhance mechanical properties. In hot extrusion, sintered metal is heated to 50-75 % of its melting temperature [4]. To avoid metal seizing, the extrusion die is heated near the metal temperature. Then, heated metal billets are extruded in a shaped extrusion die by applying an appropriate pressure. It makes the die of the conversing shape. The ratio of in to out the cross-section area of the extrusion die is known as the extrusion ratio. During the extrusion process, the material passes through a narrow opening; It suffers compressive and rheological shear loading. It axially

aligns the randomly oriented reinforced particulates and decreases the porosity content. It may facilitate densification, which significantly enhances the microstructure and mechanical properties [6]. According to the literature, extrusion ratios affect the microstructure and mechanical properties of AZ91D magnesium alloy undergoing the hot extrusion process [7,8]. It also depicts that grain refinement and interfacial adhesion have a great influence on the extrusion ratio.

Extrusion of materials through the die depends on the profile parameters and complexity of the die opening. The factor of complexity is also controlled by the applied resultant forces in the direction of flow during the process, which is variable and increases with the rise in temperature and gravitational force [1–15]. Nevertheless, complexity decreases with an increase in the profile perimeter of the die opening but also depends on the force/pressure of extrusion as well as on the ductile behavior of the material. For pure copper, the combined effect of experimental parameters such as profile of the die opening, rise in temperature, extrusion force, extrusion ratio, etc., might be the reason behind the excellent level of grain refinement and metallurgical properties [1–17].

The present work evaluated the effect of different extrusion ratios on the microstructure of sintered copper prepared by the hot extrusion process. The Cu specimens were prepared by two routes, i.e. (1) powder metallurgy route and (2) powder metallurgy route followed by hot extrusion for different extrusion ratios. Synthesized copper specimens were analyzed according to a function of extrusion ratio and metallurgical characteristics. In this work, a synergetic effect of the two-processing techniques (powder metallurgy and extrusion) has been used to improve the grain refinement and properties of pure copper specimens. This work is mostly suitable and recommended for the essential utilization of copper-based components, where the inclusion of ceramic and any type of reinforcement is not preferred.

Materials and Methods

The present study used an electrolytic copper powder, Loba Chemicals Pvt. of an average size of 40 μm and 99.9 % purity. The copper powder was preheated at 120 $^{\circ}\text{C}$ for 1.5 h to remove the moisture content from the powder and milled at 300 rpm for 1 h in a planetary ball mill.

The steps involved in the fabrication process are described in Fig. 1. Hardened steel balls were used with a ratio of 5:1 for the ball-to-powder weight ratio. In Fig. 2(a), copper powder particles are represented with some sharp edges followed by the ball milling process shown in Fig. 2(b). After milling, the copper powder was cold compacted at 700 MPa with a 3-min dwell time in a custom-made two-piece compaction die shown in Fig. 2(c), with the use of zinc stearate as the die lubricant. The green compact was sintered at 900 $^{\circ}\text{C}$ for 1.5 h in a three-stage diffusion furnace (Fig. 2(c)).

To reduce the porosity content of copper, hot extrusion was used as a secondary process after sintering (Fig. 2(d)). For the hot extrusion process, sintered billets of size 20 mm in diameter and 30 mm in height were heated up to 750 $^{\circ}\text{C}$ for 20 mins. Complex die for the extrusion consists of several parts or the load sustaining and hold for the constant die cavity space. The most important part of the extruded die part shown in Fig. 2(d) for which the dimensions of the extruded bar are 20 mm in diameter at the inlet while 7.14, 3.17, and 1.8 mm at the outlet. With this different extruded ratio, bars were

obtained. The sintered copper pallets were extruded in a preheated extrusion die, which was maintained at 700 °C. The extrusion of the copper was done for three extrusion ratios of 2.8:1, 6.3:1, and 11.1:1 with a punch speed of 1 mm/s. The purpose of using different extrusion ratios was to analyze its effect on microstructure. Graphite was duly applied to the punch and die before each experiment to carry out the extrusion process in the dedicated extrusion die. FESEM (Field Emission Scanning Electron Microscopy), EDX (Energy Dispersive X-ray), and XRD (X-ray Diffraction) analyses were conducted to identify the surface morphology, phase formation, and physical properties of the extruded specimens.

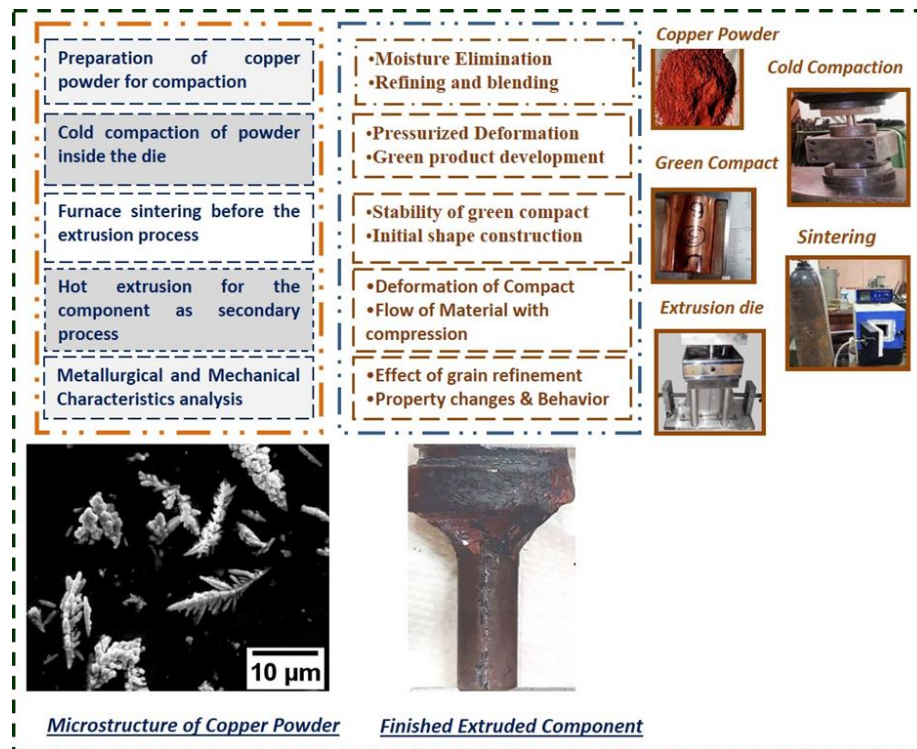


Fig. 1. Synthesis steps of Extruded copper component

The ball milling was performed at room temperature with volume size $(\pi/4) 862 \times 80 \text{ mm}^3$, RETSCH PM-100). Compressive stress evaluation was performed by the prepared sample of extruded specimens according to the ASTM E9-19 standard. For this purpose, the diameter to length ratio was maintained at 0.8. The compression test was done with the help of a UTM (Universal Testing Machine) until the first crack was developed along the lateral dimension of the specimen. It was considered the rate of the load increases constant with a value of 0.25 MPa/s. It was observed that for a limited value of load between 250 and 280 KN first fracture on the lateral surface appeared and obtained data has been reported for this work. To examine the performance of the prepared composite, well-polished samples (roughness below 0.05 μm) were used with the help of EDX attached FESEM (ZEISS, SUPRA 40 P). XRD analysis was conducted by using (PAN AlyticalXpert, K-Alpha1 wavelength: 1.540598 nm radian intensity up to 26000 a.u.) scanning range of 10-90° with a step size 0.02°/sec.

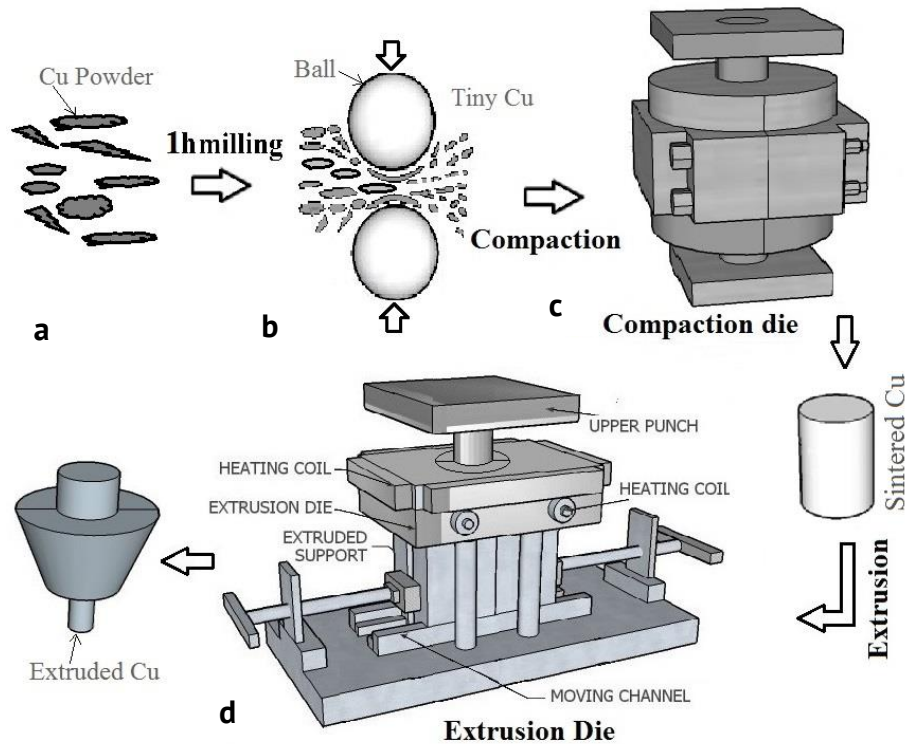


Fig. 2. Processing sequence for the synthesis of copper extruded specimen (a) Cu powder particles; (b) Ball milling process; (c) Powder compaction inside the die and sintering process; (d) representation of extrusion die process

Vicker's microindentation hardness tester (VI diamond indenter, CSM Instruments, Singapore) was used for the measurement of microhardness of the extruded pallets on different locations by a maximum load of 2000 mN with a pause time of 10-20 seconds. To the accuracy of the results, a minimum of 5 tests for each phase were conducted for different locations, and an average of the obtained values was reported. Moreover, for each indentation, a minimum indentation distance of $2.5d$ (d is indentation diameter) was maintained in each phase and experiment. For FESEM analysis, the specimens were prepared by grinding the samples with 2000-grade silicon grit paper followed by polishing with fine alumina powder. Finally, the specimens were etched with a solution of 5g FeCl₃ in 15 ml HCl and 90 C₂H₆OH to observe the grain morphology.

Results and Discussion

The density of all copper specimens is determined by the Archimedes method. Table 1 shows the value of actual density, sintered density, and relative density of copper for different extrusion ratios. Figure 3(a) shows the density of Cu and extruded Cu with different extrusion ratios. The general trend shows that the sintered density increases with increasing extrusion ratio. The narrow opening of the extrusion die may increase compressive and shear stress, which significantly increases the particle-to-particle contact and results in the close packing of the Cu particles. It may increase the density of Cu by increasing the extrusion ratio. The theoretical density of the copper is 8.96 g/cm³ [3]. The relative density of the Cu increases with increasing the extrusion ratio and achieves its

maximum value (8.66 g/cm^3) of 96.65 % at an 11.1 extrusion ratio, which is 4.9 % higher than that without the extrusion process. The micrograph shown in Fig. 4 (microstructural evaluation) also depicts that the high extrusion ratio considerably reduces the pores and voids, which increase the sintered density [3]. With increasing the extrusion ratio, dynamic recrystallization of the Cu particles increases at elevated temperatures, which results in the reduction of the oxide formation and enhances the sintered density [16].

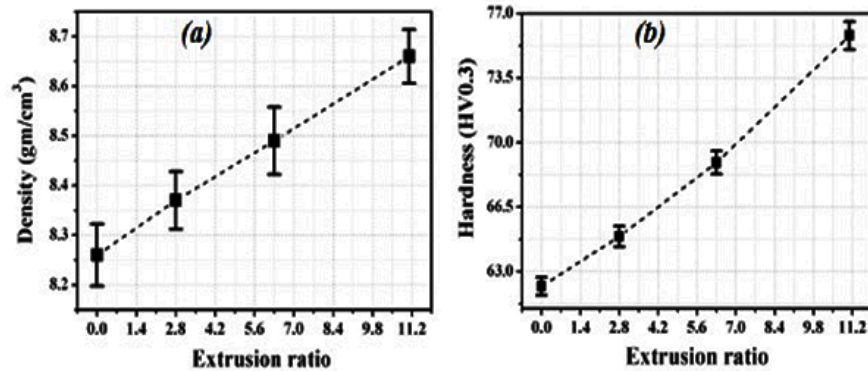


Fig. 3. (a) Variation of density with extrusion ratio, and (b) variation of hardness with extrusion ratio

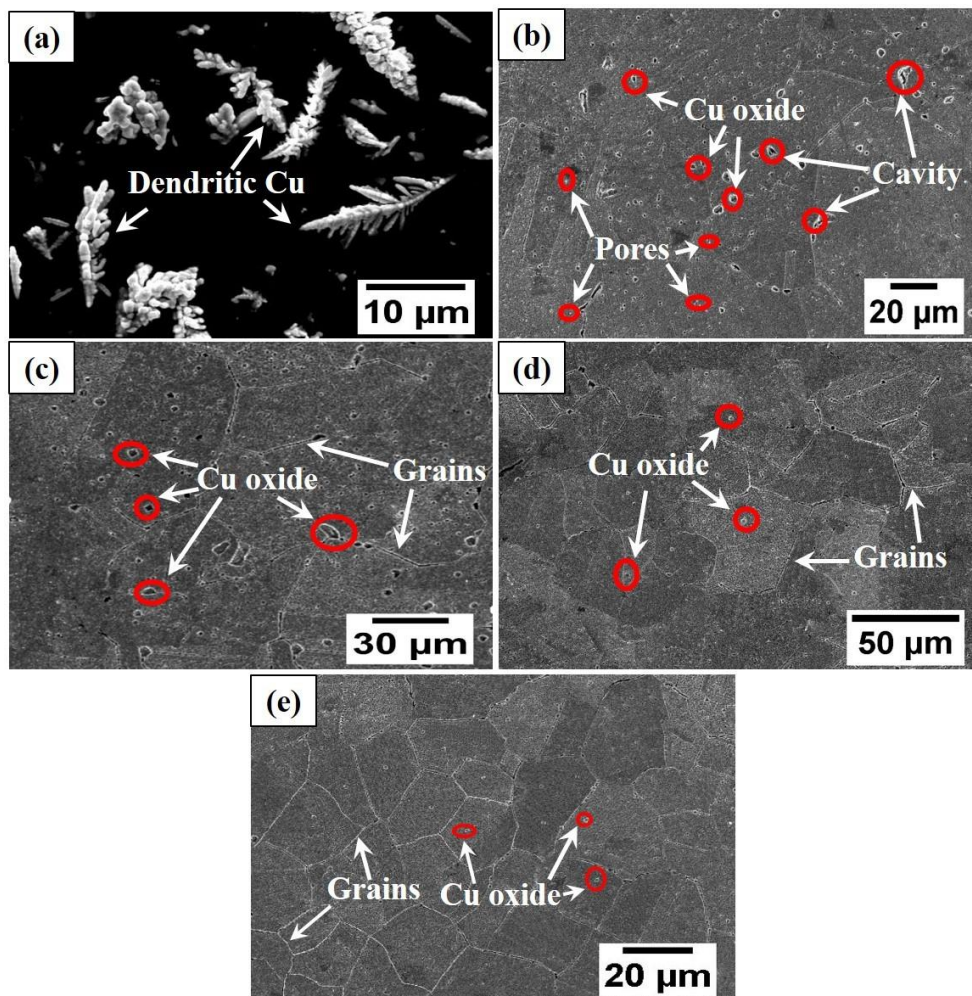


Fig. 4. FESEM images of (a) as received dendritic copper powder, (b) Cu without extrusion, (c) Cu extruded with a 2.8:1 extrusion ratio, (d) Cu with a 6.3:1 extrusion ratio, (e) Cu with an 11.1:1 extrusion ratio

Figure 3(b) shows the value of the microhardness of the Cu for different extrusion ratios. It illustrates that the value of hardness increases with increasing extrusion ratios. The hardness depends on the porosity content, interface bonding, and plastic deformation of the material at the point of indentation [15]. The micrograph (Fig. 4) shows that the porosity of the copper decreases with an increase in the extrusion ratio, with a reduction in the amount of pores.

Table 1. Relation of actual density, theoretical density, and relative density with respect to extrusion ratio

S. No.	Extruded Alloy	Actual density, g/cm ³	Theoretical density, g/cm ³	Relative density, %
1	Cu	8.26	8.96	92.12
2	Cu (2.8 ext. ratio)	8.37	8.96	93.41
3	Cu (6.3 ext. ratio)	8.49	8.96	94.75
4	Cu (11.1 ext. ratio)	8.66	8.96	96.65

It may be attributed to the strong bonding and close particle packing of Cu at a higher extrusion ratio [18–23]. With an increasing extrusion ratio, the oxide precipitate is broken into small pieces and homogeneously dispersed. A higher nucleation rate leads to dynamic recrystallization, which further leads to grain refinement [20,24–26]. In hardness tests, fine grain structure and uniform dispersion of oxide content create an obstacle in displacing the copper during the indentation of the diamond ball. This strengthening mechanism increases the hardness of the extruded copper. The hardness value of sintered copper is 62.2 HV. The value increases with the extrusion ratio and achieves its maximum value of 75.8 HV for an 11.1 extrusion ratio. Thus, the study reported a 21.9 % increase in the microhardness of Cu with an extrusion ratio of 11.1 than of without extrusion. Authors [4,12] have reported a similar result of microhardness. It was found that the value of microhardness increases from 66.2 to 77.2 VHN with an increasing extrusion ratio from 4:1 to 15:1. Generally, hardness value is a dependent parameter on the types of material such as abrasive and matrix-based material. As, in this experimental work, no abrasive has been used but due to compaction and dual sintering process, synthesized copper alloy has been denser. This results in the reduction in porosity as discussed, which also affects the micro-indentation hardness. This is a simple phenomenon for the different phases generated due to sintering and reduction of porosity [7,16].

Figure 5(a) shows the micrograph of extruded Cu for a 2.8:1 extrusion ratio. Several numbers of pores with interfaces of Cu and Cu-oxide phases are identified in Fig. 5(a). These interfaces are variable according to the size and dominated by the copper due to which variable density and porosity have been obtained as discussed earlier. For this, Fig. 5(b) shows the EDX spectra of extruded Cu with the elemental analysis. The elemental analysis of EDX spectra shows oxygen content, which may confirm the formation of copper oxide. It may be attributed to the involvement of atmospheric oxygen during the sintering and hot extrusion process [15,16]. The corresponding micrograph for the hardness test at the copper extruded surface is represented in Figs. 5(c,d) related to copper and its interfaces. These micrographs are directly affected by the elemental involvement and interfaces as observed in the EDX spectrum. Both the phases shown in Fig. 5(a,b) are different from each other according to indentation. Indentation for pure copper (Fig. 5(a)) is more uniform than the indentation in the oxide phase of copper (Fig. 5(b)).

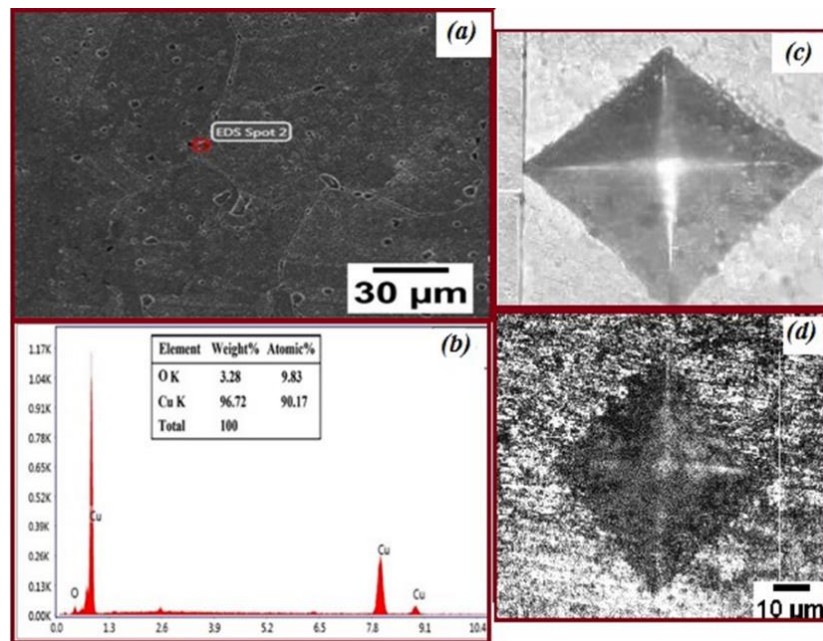


Fig. 5. (a) Micrograph of Cu extruded with the extrusion ratio of 2.8:1; (b) EDX spectrum with the elemental analysis; (c) microindentation on pure copper phase; (d) microindentation on the interface of Cu-oxide phase

The general trend in Fig. 6 depicts that electrical conductivity increases with increasing the extrusion ratio. It shows the highest value of electrical conductivity (94.9 % IACS) for the extrusion ratio of 11.1 which is 8.11 % greater than that of the Cu without extrusion. The increase in the electrical conductivity may be attributed to the reduction in porosity content with increasing the extrusion ratio. The synergetic effect of pores elimination and strong interface adhesion may remarkably enhance the electrical conductivity by increasing the extrusion ratio.

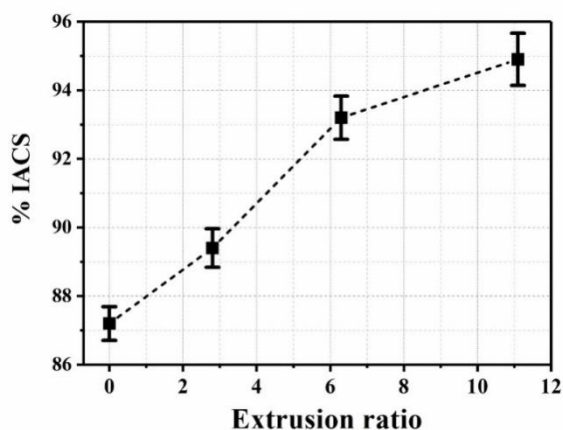


Fig. 6. Variation of electrical conductivity (% IACS) with extrusion ratio (%)

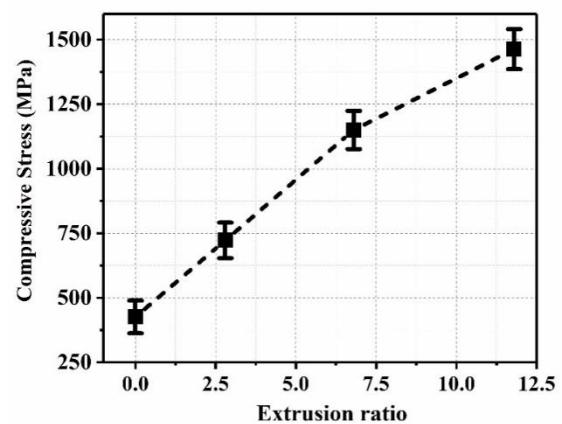


Fig. 7. Variation of compressive strength (MPa) with extrusion ratio (%)

The electrical conductivity of any material depends on several factors, including: (1) number of free electrons present; (2) porosity and cavity content; (3) interfacial adhesion of the material.

It may refer to the ease in the movement of free electrons, as the presence of pores and cavities may act as an obstacle in the motion of free electrons. It may also be attributed to strong interface adhesion with increasing the extrusion ratio, which may refer to the high plastic deformation of the Cu under high compression and shear stress at elevated temperatures [7,16]. However, the 1.79 % increase in electrical conductivity (93.2 to 94.9 % IACS) with increasing the extrusion ratio from 6.3 to 11.1 depicts less increment in the electrical at high extrusion ratio. It refers to the excellent interface adhesion and low porosity content at a 6.3 extrusion ratio, therefore less improvement is depicted in interface adhesion, and porosity content may be depicted with increasing further extrusion ratio.

The size and shape of the particles in the specimens have an impact on the compression behavior, which varies. Energy is stored in the extruded copper pallets before any first cracking and is distributed among the contact particles with the compaction surface [13,15,16,27]. As represented in Fig. 7, it seems that compressive stress values for the copper extruded billets increase with the increase in extrusion ratio. A maximum value for the compressive stress before fracture is obtained about 1442 MPa (for 11.1 extrusion ratio) which is approx. 277 % higher than the non-compressed extrusion pallets. Moreover, for the extrusion ratio of 2.8 and 6.3, the value of compressive stress reached 742 and 1156 MPa, respectively. These obtained results show the combined effect of extrusion ratio and initial compaction with grain refinement for copper pallets. When a compressive force is applied, internal fracture (dislocation) initiation for copper billets is always started within grains, moving toward the grain boundary. As Copper has a high work hardening exponent and these dislocations pile up and immediately form a dislocation forest (Frank–Read source). These dislocation forests may accumulate at the grain boundaries. As interaction of the two dislocations are repulsive in nature. Therefore, more compressive stress is required to propagate the dislocation from the grain boundaries, as the dislocation forest present at the grain boundary may create obstacles in the movement of dislocation. A high extrusion ratio increases the number of grains present in the same region, which leads to more compressive stress to propagate the dislocation from these grain boundaries [16]. In the compression test, dislocations (cracks) are initiated within the material and progressively moved towards the outer direction. At an optimum value of compressive stress, these dislocations (cracks) may come out from the material surface and cause the first fracture on the specimen's outer lateral surface. Therefore, grain refinement may increase the compressive strength of the extruded copper by increasing the extrusion ratio.

Figure 4 shows the micrographs of the sintered Cu and the sintered Cu extruded for different extrusion ratios. The metallographic images are taken perpendicular to the extrusion direction. With an increasing extrusion ratio, the micrograph in Fig. 4 shows the recrystallization of Cu with a more refined and homogeneous grain structure and size. Figure 4(a) depicts the dendritic shape of received the copper. It shows an extended facet of dendritic copper. Figure 4(b) illustrates the micrograph of copper sintered at 900 °C. It shows non-uniform grains of large size along with the formation of copper oxide (CuO). The micrograph shows some tiny pores [16,27,28].

Figure 4(c) shows the micrograph of extruded Cu with the 2.8:1 extrusion ratio. It shows the partial recrystallization with a non-uniform grain structure. It confirms that grains are suppressed however, the formation of copper oxide is observed. These oxides are marked in the micrographs (Fig. 4), mostly white phases, and settled on the spaces available between

grains and pores. The reduction in grain size may refer to densification during extrusion [27]. The micrograph in Fig. 4(d) shows the extruded Cu with the 6.3:1 extrusion ratio. It shows the recrystallization along with the non-uniform grain structure. Figure 4(d) shows that the grains are considerably suppressed along with partial grain refinement. During the extrusion process, the Cu particles pass through the confined narrow opening, which leads to achieving close particle packing [15]. It may reduce the porosity and grain size. Here, in different magnifications of the micrographs, pores size is also variable with the grain size. It can be observed from these images that the number of available pores is also variable and reduces with the increase of the extrusion ratio. The micrograph also confirms the reduction in the size of copper oxide. It may be attributed to the compressive and shear stress developed during hot extrusion, which breaks the copper oxide into small pieces [10]. Figure 7(e) shows the micrograph of extruded Cu with the 11.1:1 extrusion ratio. A high extrusion ratio may rearrange particles that may cause high plastic deformation [16].

The severe plastic deformation at elevated temperatures may store the internal energy and the system becomes thermodynamically unstable [28–30]. The micrograph in Fig. 4(d,e) shows that the porosity and cavity content decreases with increasing the extrusion ratio, concerning Fig. 4(b,c). It may lead to dynamic recrystallization and refine grain structure [1,31,32]. It may lead to a considerable reduction in grain size. Figure 4(e) shows the tiny copper oxide along with fine grain boundaries. It may refer to the development of high compressive and shear stress at a high extrusion ratio. It may break the large-size CuO into small pieces [10]. The high extrusion ratio enhances the high plastic deformation, which increases the nucleation rate [11,15,32,33]. It may be attributed to the fine grain structure at 11.1 extrusion ratio. It may eliminate porosity and enhance densification behavior.

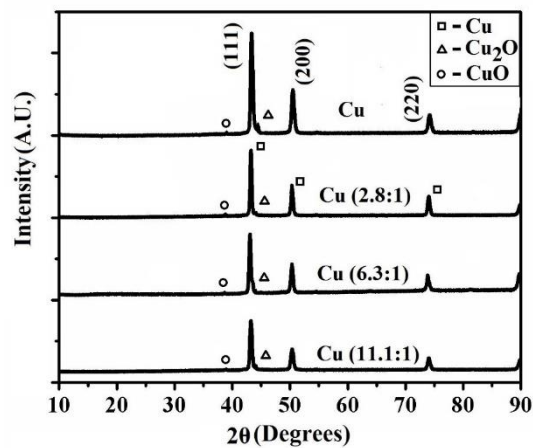


Fig. 8. XRD pattern for sintered Cu and Cu extruded with different (2.8:1, 6.3:1, and 11.1:1) extrusion ratios

Figure 8 shows the XRD pattern of Cu and extruded Cu with different extrusion ratios. XRD spectra show the intensity peaks of Cu. The interlayer lattice spacings of the Cu specimens for different extrusion ratios were determined by Bragg's law ($d = n\lambda/2\sin\vartheta$), where $n=1$, wavelength $\lambda=1.5406 \text{ \AA}$ for Cu K α , and ϑ is the Bragg angle. Figure 5 depicts the high-intensity diffraction peaks of Cu at the 2ϑ angle of 43.20 ± 0.04 , 50.26 ± 0.06 , and $73.98 \pm 0.6^\circ$ which corresponds to the lattice spacing 2.094 , 1.814 , and 1.28 \AA , respectively. This lattice spacing refer to the (111), (200), and (220) planes of the fcc Cu.

It also confirms the low-intensity peaks of CuO and Cu₂O. It may be because of the involvement of atmospheric air during sintering and the hot extrusion process. Not only that, but it reacts with the amount of oxygen present in the air with the copper at elevated temperatures and forms copper oxide [16]. The XRD pattern shows that the intensity of oxide peaks decreases with increasing the extrusion ratio. It may be attributed to grain refinement and breaking of copper oxide under high compressive and shear stress [9].

Conclusions

The sintered copper specimens were successfully extruded for 2.8, 6.3, and 11.1 extrusion ratios by hot extrusion route. Microstructure and phase formation of Cu specimens are characterized by FESEM, EDX, and XRD techniques.

The micrograph of the sintered copper shows the large grain size. It also shows oxide participation and porosity content. For a high extrusion ratio of 11.1:1, the micrograph confirms the refined and uniform grain structure with reduced oxide precipitate.

It might be attributed to high nucleation rate and dynamic recrystallization because of high compressive and shear stress at elevated temperatures. Thus, the test results recommend that the 11:1 extrusion ratio is suitable for achieving superior grain structure and mechanical properties.

The strengthening of Cu is the coordination of dynamic recrystallization, grain refinement, and homogeneous dispersion of oxide precipitates.

Obtained results for the density, compressive strength, microhardness, and electrical conductivity confirm an appreciable increase due to the effect of compression and as a function of extrusion ratio.

References

1. Liang C, Ma M, Zhang D. Microstructures and Tensile Mechanical Properties of Consolidated Copper. *Materials Research*. 2015;18: 158–163.
2. Tuncer N, Bose A. Solid-State Metal Additive Manufacturing: A Review. *JOM*. 2020;72(9): 3090–3111.
3. Yang Y, Tang S, Wang Y, Yang L, Fan Z. Process optimization of porous Al₂O₃ filter via layered extrusion forming. *Materials and Manufacturing Processes*. 2022;37(14): 1630–1641.
4. Romero C, Yang F, Raynova S, Bolzoni L. Thermomechanically processed powder metallurgy Ti-5Fe alloy: Effect of microstructure, texture, Fe partitioning and residual porosity on tensile and fatigue behaviour. *Materialia*. 2021;20: 101254.
5. Ramesh C, Hirianiah A, Harishanad KS, Noronha NP. A review on hot extrusion of Metal Matrix Composites (MMC's). *Research Inventory: International Journal of Engineering Science*. 2012;1(10): 30–35.
6. Gonzalez-Gutierrez J, Cano S, Ecker JV, Kitzmantel M, Arbeiter F, Kukla C, Holzer C. Bending Properties of Lightweight Copper Specimens with Different Infill Patterns Produced by Material Extrusion Additive Manufacturing, Solvent Debinding and Sintering. *Applied Sciences*. 2021;11(16): 7262.
7. Xin L, Yang W, Zhao Q, Dong R, Liang X, Xiu Z, Hussain M, Wu G. Effect of extrusion treatment on the microstructure and mechanical behavior of SiC nanowires reinforced Al matrix composites. *Materials Science and Engineering A*. 2017;682: 38–44.
8. Kumar P, Panda SS. A review on properties and microstructure of micro-extruded product using SPD and as-cast material. *Sādhanā*. 2018;43(5): 77.
9. Torralba JM, Alvarado P, García-Junceda A. High-entropy alloys fabricated via powder metallurgy. A critical review. *Powder Metallurgy*. 2019;62(2): 84–114.
10. Hu M, Ji Z, Chen X. Effect of extrusion ratio on microstructure and mechanical properties of AZ91D magnesium alloy recycled from scraps by hot extrusion. *Transactions of Nonferrous Metals Society of China*. 2010;20(6): 987–991.
11. Ebrahimi R, Rahimzadeh Lotfabad F. Simple shear extrusion as an efficient severe plastic deformation technique: a review. *Materials Science and Technology*. 2022;39(3): 259–282.
12. Ramesh CS, Keshavamurthy R, Naveen GJ. Effect of extrusion ratio on wear behaviour of hot extruded

- Al6061–SiCp (Ni–P coated) composites. *Wear*. 2011;271(9-10): 1868–1877.
13. Wilson MF, Donaldson IW, Bishop DP. Sinter-swage processing of an Al-Si-Mg-Cu powder metallurgy alloy. *Canadian Metallurgical Quarterly*. 2022;61(1): 94–107.
 14. Zhang T, Ji Z, Wu S. Effect of extrusion ratio on mechanical and corrosion properties of AZ31B alloys prepared by a solid recycling process. *Materials in Engineering*. 2011;32(5): 2742–2748.
 15. Qamar SZ. Shape Complexity, Metal Flow, and Dead Metal Zone in Cold Extrusion. *Materials and Manufacturing Processes*. 2010;25(12): 1454–1461.
 16. Dixit M, Srivastava R. The effect of copper granules on interfacial bonding and properties of the copper-graphite composite prepared by flake powder metallurgy. *Advanced Powder Technology*. 2019;30(12): 3067–3078.
 17. Pilz F, Merklein M. Influence of component design on extrusion processes in sheet-bulk metal forming. *International Journal of Material Forming*. 2019;13: 981–992.
 18. Ji X, Zhang H, Luo S, Jiang F, Fu D. Microstructures and properties of Al–Mg–Si alloy overhead conductor by horizontal continuous casting and continuous extrusion forming process. *Materials Science and Engineering: A*. 2016;649: 128–134.
 19. Basinski ZS, Dugdale JS, Howie A. The electrical resistivity of dislocations. *Philosophical Magazine*. 1963;8(96): 1989–1997.
 20. Dixit M, Srivastava R. Effect of compaction pressure on microstructure, density and hardness of Copper prepared by Powder Metallurgy route. *IOP Conference Series: Materials Science and Engineering*. 2018;377: 012209.
 21. Wu Y, Li Y, Lu J, Tan S, Jiang F, Sun J. Correlations between microstructures and properties of Cu-Ni-Si-Cr alloy. *Materials Science and Engineering: A*. 2018;731: 403–412.
 22. Liu Y, Cai S, Xu F, Wang Y, Dai L. Enhancing strength without compromising ductility in copper by combining extrusion machining and heat treatment. *Journal of Materials Processing Technology*. 2019;267: 52–60.
 23. Wang J, Feng Z. Manufacturing of surface features from extrusion forging and extrusion rolling of sheet metals. *Manufacturing Letters*. 2018;15: 42–45.
 24. Geißdörfer S, Rosochowski A, Olejnik L, Engel U, Richert M. Micro-extrusion of ultrafine grained copper. *International Journal of Material Forming*. 2008;1: 455–458.
 25. Wu Y, Huang S, Chen Q, Feng B, Shu D, Huang Z. Microstructure and Mechanical Properties of Copper Billets Fabricated by the Repetitive Extrusion and Free Forging Process. *Journal of Materials Engineering and Performance*. 2019;28(4): 2063–2070.
 26. Wang M, Averback RS, Bellon P, Dillon S. Chemical mixing and self-organization of Nb precipitates in Cu during severe plastic deformation. *Acta Materialia*. 2014;62: 276–285.
 27. Selmi O, Hamza Bouzid, Saidi H, Abdelaziz Bouazizi. The effect of copper doping on the optical and electrical properties of nickel oxide thin films deposited by spin coating technique. *Emergent Materials*. 2021;5(4): 1033–1038.
 28. Agarwal M, Srivastava R. Effect of thick slurry and stepped deformation on mechanical properties of AA6061 alloy. *Emerging Materials Research*. 2019;8(3):394–403.
 29. Agarwal M, Dixit NK, Dixit M, Srivastava R. Interfacial study for the effect of Al₂O₃ addition on the microstructure and micro-hardness of the Al₂O₃/AA6061 semi-solid cast composite. *Phase Transitions*. 2021;94(12): 899–909.
 30. Meignanamoorthy M, Ravichandran M. Synthesis, properties and microstructure of sintered and hot extruded boron carbide reinforced AA8079 (Al-Cu-Fe-Si-Zn) matrix composites. *Materials Research Express*. 2018;5(11): 116508.
 31. Musabirov II, Safarov IM, Galeev RM, Afonichev DD, Koledov VV, Rudskoy A, Mulyukov RR. Plastic deformation of the Ni-Mn-Ga alloy by multiple isothermal forging. *Materials Physics and Mechanics*. 2017;57(1): 124–136.
 32. Chen J, Yang CL, Yan W, Xia F, Fan X. Effect of Transverse Grain Boundary on Microstructure, Texture and Mechanical Properties of Drawn Copper Wires. *Journal of Materials Science and Technology*. 2014;30(2): 184–191.
 33. Andreev AP, Andreeva SI, Shibakov VG, Pankratov DL. The heterogeneity of the stress-strain state during severe plastic deformation by multiple extrusion. *Materials Physics and Mechanics*. 2015;22(2): 170-175.

About Authors

Abbas Mehdi

M. Tech Scholar (B.N. College of Engineering and Technology, Lucknow, India)

Manish Dixit Sc

PhD, Associate Professor (B.N. College of Engineering and Technology, Lucknow, India)

Mayank Agarwal Sc

PhD, Associate Professor (Dr. RML Avadh University, Faizabad, India)